PNAS

Supporting Information for

XCR1 expression distinguishes human conventional dendritic cells type 1 with full effector functions from their immediate precursors

Lukas Heger[1*], Lukas Hatscher[1], Chunguang Liang[2], Christian H. K. Lehmann[1,3], Lukas Amon[1], Jennifer J. Lühr[3], Tomasz Kaszubowski[1], Rayk Nzirorera[1], Niels Schaft[5,6,7], Jan Dörrie[5,6,7], Pascal Irrgang[8], Matthias Tenbusch[3,8], Meik Kunz[2,9,10], Eileen Socher[11], Stella E. Autenrieth[12], Ariawan Purbojo[13], Horia Sirbu[14], Arndt Hartmann[15], Christoph Alexiou[16], Robert Cesnjevar[13,17], and Diana Dudziak[1,3,5,6*]

[1] Department of Dermatology, Laboratory of Dendritic Cell Biology, Friedrich-Alexander-Universität Erlangen-Nürnberg (FAU), Universitätsklinikum Erlangen, Erlangen, Germany

[2] Chair of Medical Informatics, FAU, Erlangen, Germany

[3] Medical Immunology Campus Erlangen, Erlangen, Germany

[4] Nano-Optics, Max Planck Institute for the Science of Light, Erlangen, Germany

[5] Department of Dermatology, RNA-based immunotherapy, FAU, Universitätsklinikum Erlangen, Erlangen, Germany

[6] Deutsches Zentrum Immuntherapie (DZI), 91054 Erlangen

[7] Comprehensive Cancer Center Erlangen-European Metropolitan Area of Nuremberg (CCC ER-EMN), Erlangen, Germany

[8] Institute of Clinical and Molecular Virology, FAU, Universitätsklinikum Erlangen, Erlangen, Germany

[9] Fraunhofer Institute for Toxicology and Experimental Medicine (ITEM), Hannover, Germany

[10] Fraunhofer Cluster of Excellence Immune-Mediated Diseases (CIMD), Hannover, Germany

[11] Functional and Clinical Anatomy, Institute of Anatomy, FAU, Erlangen, Germany

[12] Research Group “Dendritic Cells in Infection and Cancer” (F171), German Cancer Research Center (DKFZ), Heidelberg, Germany

[13] Department of Pediatric Cardiac Surgery, FAU, Universitätsklinikum Erlangen, Erlangen, Germany

[14] Department of Thoracic Surgery, FAU; Universitätsklinikum Erlangen, Erlangen, Germany

[15] Department of Pathology, FAU, Universitätsklinikum Erlangen, Erlangen, Germany

[16] Department of Otorhinolaryngoly, Section of Experimental Oncology and Nanomedicine, FAU, Universitätsklinikum Erlangen, Erlangen, Germany

[17] Department of Pediatric Cardiac Surgery, University Zurich, Zurich, Switzerland

* corresponding authors: Diana Dudziak; Lukas Heger
Email: diana.dudziak@uk-erlangen.de; lukas.heger@uk-erlangen.de

This PDF file includes:

Supporting Information text
Figures S1 to S11
Tables S1 to S5
SI References

Supporting Information text

Methods

Cross-priming assays

CD8$^+$ T cells and DC subpopulations were isolated from PBMCs of HLA-A2$^+$ healthy donors. DCs were enriched and isolated as described above. CD8$^+$ T cells were isolated using the EasySep Human CD8+ T Cell Isolation Kit (Stemcell Technologies) as described in the manufacturer's instructions. Isolated CD8$^+$ T cells were then electroporated with mRNA encoding a TCR that is specific for the HLA-A*02:01-resticted gp100-peptide YLEPGPVTA. The electroporation was performed as described before(1–3). Briefly, RNA encoding the gp100/HLA-A*02:01-specific TCR was transcribed *in vitro* from a linearized plasmid template. The *in vitro* transcription was performed with T7 RNA polymerase (mMESSAGE mMACHINE T7 Ultra kit; Ambion, Austin, TX, USA) according to the manufacturer's instructions. The transcribed RNA was recovered using RNeasy columns (Qiagen GmbH, Hilden, Germany) according to the manufacturer's instructions. For electroporation, CD8$^+$ T cells were resuspended in OptiMEM at a concentration of $8*10^7$/ml. RNA was transferred to a 4-mm cuvette (Peqlab, Erlangen, Germany) (150 µg/ml final concentration). A volume of 100–600 µl of cell suspension was added and pulsed in a Genepulser Xcell (Bio-Rad, Munich, Germany). Pulse conditions were square-wave pulse, 500 V, 5 ms. CD8$^+$ T cells were then resuspended in T cell medium. After incubation for 4h at 37°C, T cells were harvested and co-cultured with sorted DC subpopulations in a 1:1 ratio. Before the co-culture, DCs were fed either with a long or short gp100-peptide and stimulated with 5µg/ml pIC and R848 for 3h. After 18 and 36h of co-cultivation, T cells were analyzed for the expression of CD69 and CD25 by flow cytometry and the supernatant was analyzed for the secretion of IFNγ, IL-2, and TNF by CBA assay (BD Biosciences). Acquisition of the samples was performed using a BD LSRFortessa and data were analyzed using FlowJo (CD69, CD25) or FCAP Array v3.0 software (BD Bioscience; cytokine secretion).

Mixed leukocyte reactions

Naïve CD4$^+$ or CD8$^+$ T cells were isolated with EasySep Human Naïve CD4+ T Cell Isolation Kit II (Stemcell Technologies) or EasySep Human Naïve CD8+ T Cell Isolation Kit II (Stemcell Technologies), respectively, as described in the manufacturer's instruction. Purified T cells were labeled with CFSE (5µM; Life Technologies) for 15min at 37°C. Afterwards T cells and DCs of HLA-mismatched donors were co-cultured in different ratios. DCs were stimulated either with R848 (1µg/ml) or pIC (1µg/ml). After 6 days, T cells were restimulated with 50ng/ml PMA and 500ng/ml Ionomycin for 6h in presence of 5µg/ml Brefeldin A. Subsequently, T cells were harvested and stained for flow cytometric analysis. For exclusion of dead cells, cells were firstly stained with Zombie UV dye (BioLegend) for 15min at 4°C. Then, cells were extracellularly stained for T cell (CD3, CD4, CD8) as well as activation (CD25) markers for 15min at 4°C. Afterwards, cells were fixed using Cytofix/Cypoperm (BD Biosciences) for 15min at 4°C and intracellularly stained for IL-2 (PE/Dazzle594, clone: MQ1-17H12, BioLegend), IL-4 (CD4$^+$ T cells only; A647, clone: 8D4-8, Biolegend), IL-10 (CD4$^+$ T cells only; PE, clone: JES3-9D7, BioLegend), IL-17A (CD4$^+$ T cells only; BV605, clone: BL168, BioLegend), IFNγ (BV421, clone: 4S.B3, BioLegend), and TNFα (PE/Cy7, clone: MAb11, BioLegend) for 30min at RT. Acquisition of the samples was performed using a BD LSRFortessa and data were analyzed using FlowJo.

Nanostring assay

XCR1+ and XCR1- cDC1 were sorted from PBMCs of healthy donors as described above. Afterwards, cells were stimulated for 3h at 37°C with 5µg/ml R848 or control treated. Then, cells were lysed in 1/3 RLT buffer (Qiagen) and sample mRNAs were stored at -80°C until further analysis. Nanostring assay with the nCounter® Human Myeloid Innate Immunity V2 Panel (NanoString Technologies) with 30 additional genes (CASP4, CASP8, NLRP1, NLRP12, NLRC4, NAIP, AIM2, MEFV, GSDMD, ANPEP, IFNL1, IFNL2, IFNL3, CADM1, NLRC5, RAB15, ZNF366,

CD226, TEAD4, TCF7L2, EPAS1, LHX6, TCF7, CLNK, C1ORF54, ABCA1, ZBTB32, GZMK, AXL, SIGLEC6) was performed using manufacturer's instructions. In brief, samples were thawed and put into a thermal cycler for hybridization with reporter code sets (target-specific Reporter and Capture Probes) for 24h. Reporter code sets consist of many RNA capture probes targeting specific mRNAs. Each probe is labeled with a unique combination of fluorochromes (molecular barcode). Therefore, specific mRNAs can be detected and counted after hybridization using the nCounter® System. Data were subsequently analyzed and exported using the nSolver software (version 4.0, NanoString Technologies). Data were further processed with RUVg (76) to remove unwanted variation. Eventually, they were analyzed in R using NanoStringNorm (77) and edgeR (78), and DEGs were determined with a threshold of false discovery rate (FDR)– Benjamini-Hochberg adjusted P value of 0.01 and a log2 fold change (FC) of 1.5.

DC-NK cell co-culture

For co-culture experiments with DCs and NK cells, DCs and NK cells were sorted from PBMCs of healthy donors. DCs were FACS-sorted as described above. NK cells were enriched from PBMCs by the depletion of unwanted cells. Therefore, PBCMs were incubated with biotinylated antibodies against CD3 (clone: SK7, BioLegend), CD8 (clone: RPA-T8, BioLegend), CD19 (clone: HIB19, BD Biosciences), CD89 (clone: A59, BioLegend), CD235a (clone: HIR2, Thermo Fisher Scientific), and HLA-DR (L243, BD Biosciences). Antibody-bound cells were magnetically labeled with MoJo Streptavidin Nanobeads (BioLegend) for 15min at 4°C and depleted by incubation inside "The Big Easy" EasySep Magnet (Stemcell Technologies) for 5min at RT. The remaining cells were stained with CD3-BV605 (clone: UCHT-1, BioLegend), CD19-BV605 (clone: SJ25C1, BioLegend), CD20-BV605 (clone: 2H7, BioLegend), HLA-DR-BV510 (clone: L243, BioLegend), CD56-BV421 (clone: 5.1H11, BioLegend) and NKp46-BV421 (clone: 9E2, BioLegend) and sorted as $CD56^{+}NKp46^{+}CD3^{-}CD19^{-}CD20^{-}HLA\text{-}DR^{-}$ cells. DCs and NK cells were co-cultured in a 1:5 ratio and either stimulated with a cocktail of pIC (2.5µg/ml), R848 (2.5µg/ml) and CpG (2.5µg/ml) or cultured in DC-medium alone. For some experiments, DCs and NK cells were separated in Transwell plates (96 well, 0.4µm insert). NK cells were cultured in the well, while DCs were added to insert. In order to analyze the influence of secreted cytokines on NK cells, NK cells were cultured alone and supernatants of stimulated DCs were added corresponding to a 1:5 DC:NK cell ratio. After 18h, cells were harvested and analyzed by flow cytometry for activation of NK cells (CD69). The supernatants were stored at -80°C until analysis with LEGENDplex Human Interferon Panel (BioLegend) for secretion of IFNγ.

Figures S1 to S11

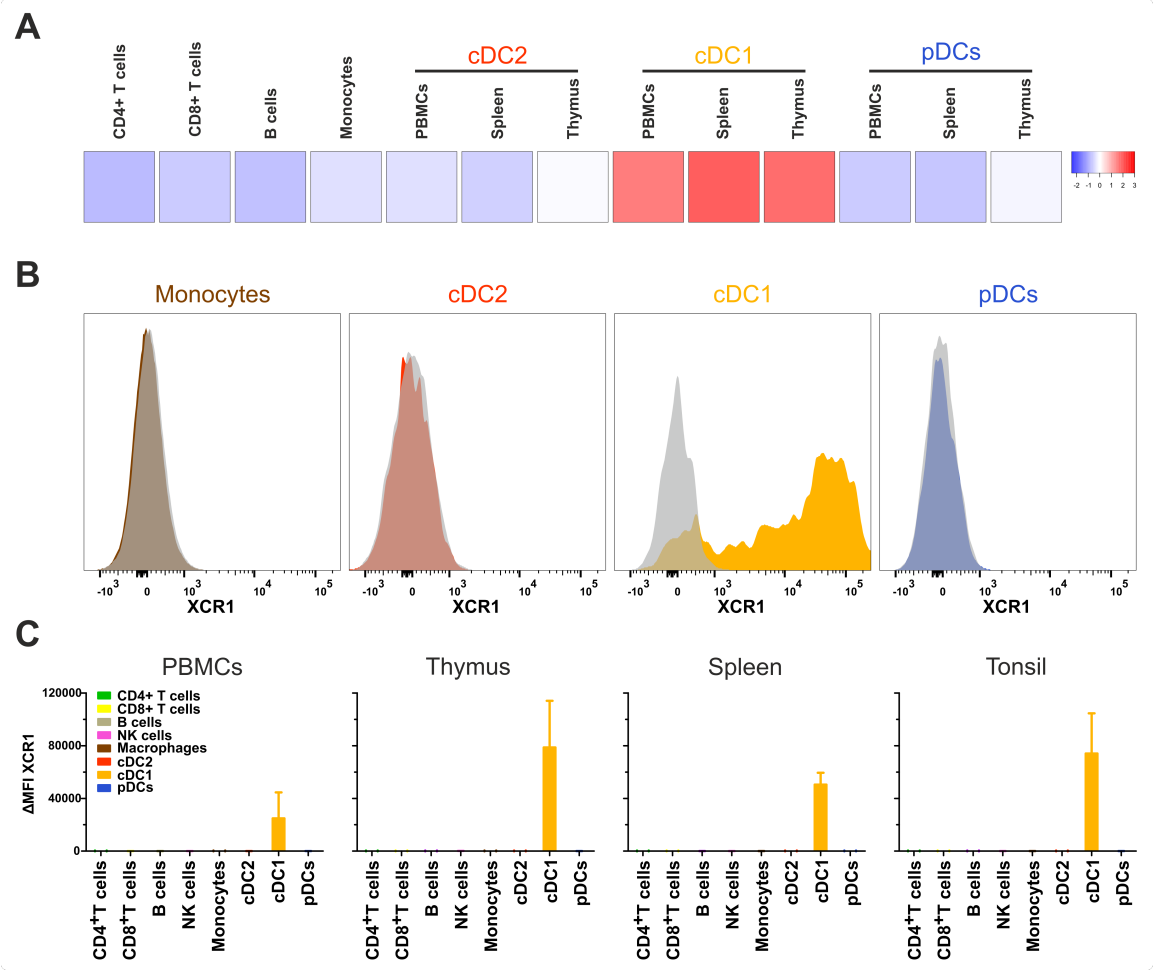

Fig. S1. Selective expression of XCR1 on human cDC1 in different lymphohematopoietic tissues. A) Previously published whole human Agilent microarray data [(12), (GEO accession number GSE77671)] of sorted human cDC2, cDC1 and pDCs of PBMCs, splenic or thymic single cell suspensions as well as CD14⁺ monocytes, B cells, CD4⁺ and CD8⁺ T cells from human blood were analyzed by heatmap analysis. Shown is the expression of XCR1. Log2-transformed expression values were z-transformed and scaled to a minimum of −2 and a maximum of 2. B and C) Single cell suspensions were prepared from human blood as well as splenic, thymic, and tonsillar tissue and flow cytometrically were analyzed for XCR1 expression using PE-coupled anti-XCR1 antibody (clone: S15046E, BioLegend) or the appropriate isotype control. Cells were acquired using a BD LSRFortessa and data analyzed using FlowJo. For the analysis, cells were gated as shown in Fig. S1. B) Shown is a representative blood donor as histogram overlay (colored: anti-XCR1 antibody; grey-transparent: isotype control) for monocytes (brown), cDC2 (red), cDC1 (yellow-orange), and pDC (blue). C) Bar graphs depict the ΔMFI (MFI antibody - MFI isotype control) + standard deviation (SD) for five donors.

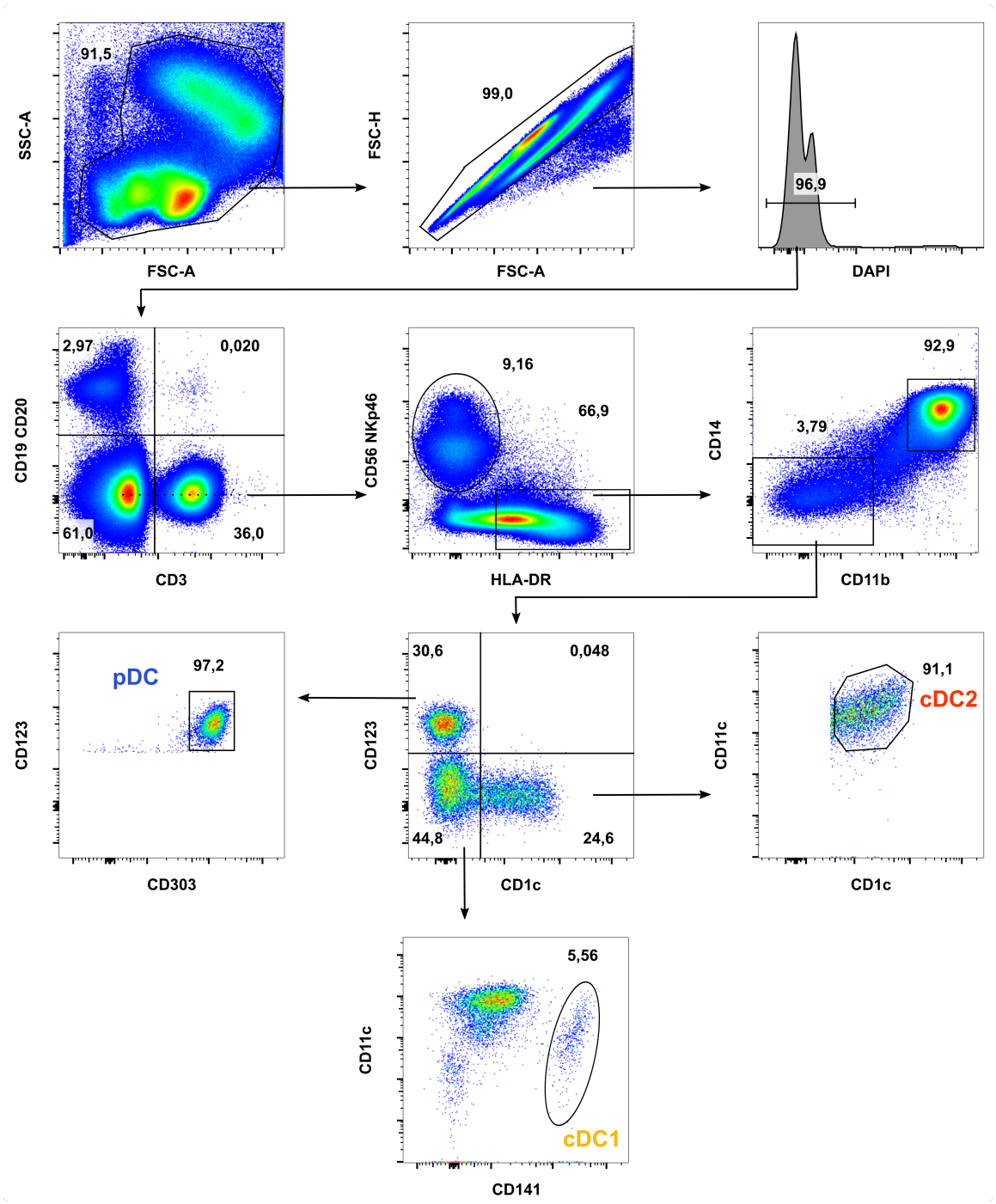

Fig. S2. Gating strategy for the flow cytometric analysis of human DC subpopulations. A representative gating strategy of one blood donor is shown. 5*10^6 PBMCs of a healthy donor were stained with fluorochrome-coupled antibodies. 1.5*10^6 cells were acquired using a BD LSRFortessa and data analyzed using FlowJo software. For the identification of human DC subpopulations, cells were gated for the morphology of leukocytes (FSC-A/SSC-A) followed by exclusion of cell doublets (FSC-A/FSC-H). From living cells (DAPI-), T cells ($CD3^+$) and B cells ($CD19/CD20^+$) were excluded. In the remaining cells, APCs ($HLA\text{-}DR^+$) not expressing NK cell marker (CD56/CD335) were selected. Monocytes were distinguished from DCs by CD11b and CD14 expression. In the $CD11b^-CD14^-$ cells, DCs were segregated into $CD1c^+CD123^-$ cells, $CD1c^-$

$CD123^+$ cells, and $CD1c^-CD123^-$ cells using a quadrant gate. In the $CD1c^+CD123^-$ compartment, cDC2 were defined as $CD1c^+CD11c^+$ cells. In the $CD1c^-CD123^+$ compartment, pDCs were identified as $CD303^+CD123^+$ cells. In the $CD1c^-CD123^-$ compartment, cDC1 were gated as $CD141^+CD11c^{int}$ cells.

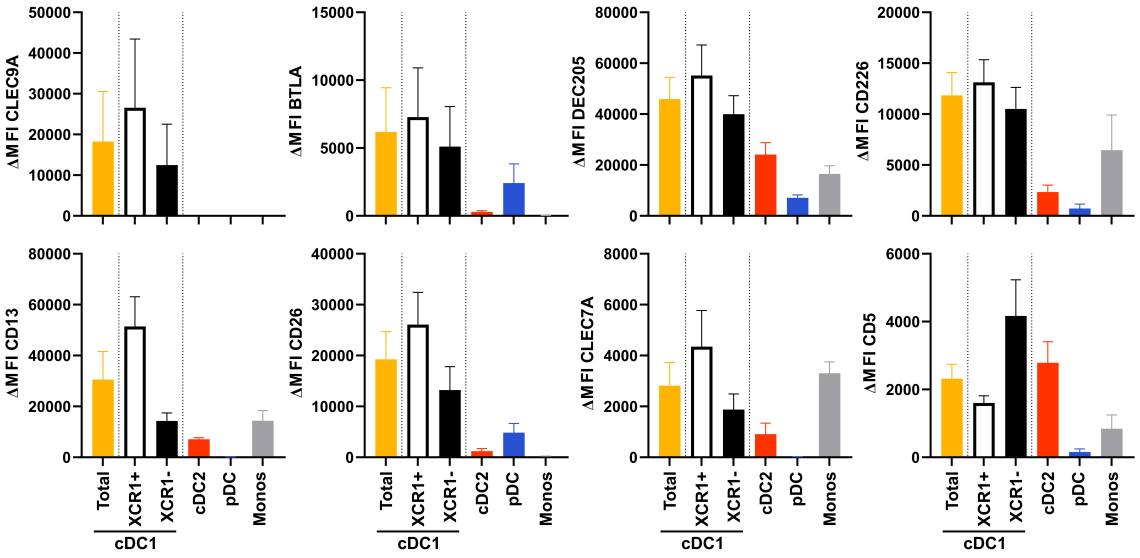

Fig. S3. XCR1$^-$ and XCR1$^+$ cDC1 show comparable expression of cDC1-associated surface markers. 5*10^6 PBMCs of a healthy donor were stained with fluorochrome-coupled antibodies (Table S5). 1.5*10^6 cells were acquired using a BD LSRFortessa and data analyzed using FlowJo software. Cells were gated according to Fig. S2 and total cDC1 (yellow-orange) additionally subdivided into XCR1$^-$ (black) and XCR1$^+$ (white) cDC1 as shown in Figure 1b. Expression of cDC1-associated surface markers CLEC9A (clone: 8F9, PE, BioLegend), BTLA (clone: MIH26, PE/Cy5, BioLegend), DEC205 (clone: MG38, PE, BD Biosciences), CD226 (clone: 11A8, PE, BioLegend), CD13 (clone: WM15, PE, BioLegend), CD26 (clone: BA5b, PE, BioLegend), CLEC7A (clone: 15E2, PE, BioLegend), and CD5 (clone: UCHT2, PE, BioLegend) were analyzed in comparison to respective isotype controls. Bar graphs show ΔMFI (mean±SD; N=5) for total cDC1, XCR1$^+$ cDC1, XCR1$^-$ cDC1, cDC2, pDC, and CD14$^+$ monocytes.

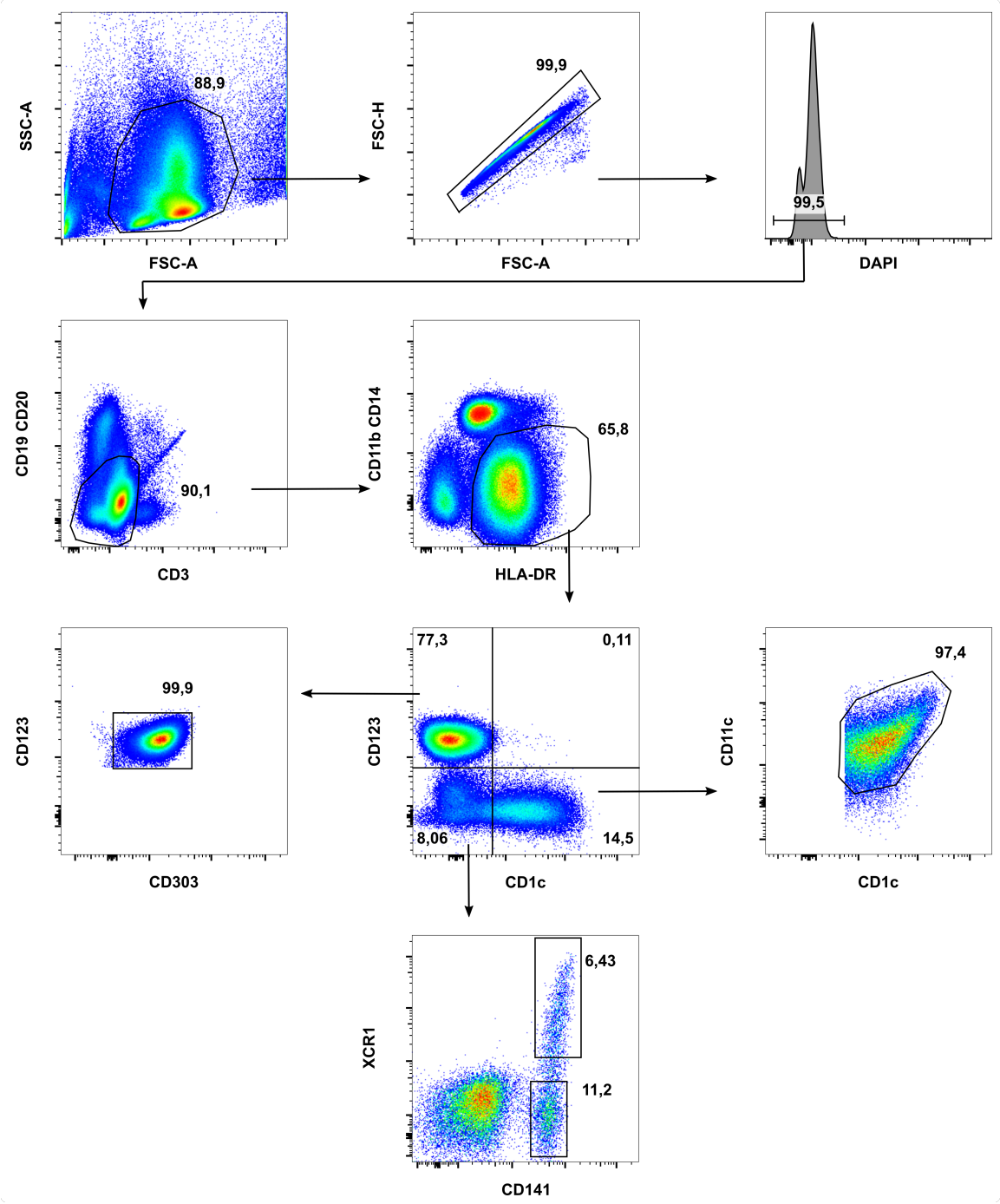

Fig. S4. Gating strategy for the isolation of XCR1$^-$ and XCR1$^+$ cDC1 by flow cytometric cell sorting. A representative gating strategy for the isolation of XCR1$^-$ and XCR1$^+$ cDC1 of one blood donor is shown. PBMCs of a healthy donor were enriched using the Pan-DC Pre-Enrichment Kit and subsequently stained with fluorochrome-coupled antibodies. Subsequently, cells were acquired using a BD FACSARIA II SORP cell sorter (70 µm nozzle, 4-way purity). After a morphology gate for leukocytes (FSC-A/SSC-A), doublets (FSC-A/FSCH-H) and dead cells (DAPI$^+$) were excluded. Remaining T cells (CD3$^+$) and B cells (CD19/CD20$^+$) were excluded. HLA-DR$^+$CD11bCD14$^-$ cells were selected and segregated into CD1c$^+$CD123$^-$, CD1c$^-$CD123$^+$, and CD1c$^-$CD123$^-$ cells. In the CD1c$^+$CD123$^-$ compartment, cDC2 were sorted as CD1c$^+$CD11c$^+$ cells. In the CD1c$^-$CD123$^+$ compartment, pDCs were sorted as CD303$^+$CD123$^+$ cells. In the CD1c$^-$CD123$^-$

compartment, XCR1$^-$ cDC1 were sorted as CD141$^+$XCR1$^-$ cells, while XCR1$^+$ cDC1 were sorted as CD141$^+$XCR1$^+$ cells. Purity of the isolated cells was routinely above 95 %.

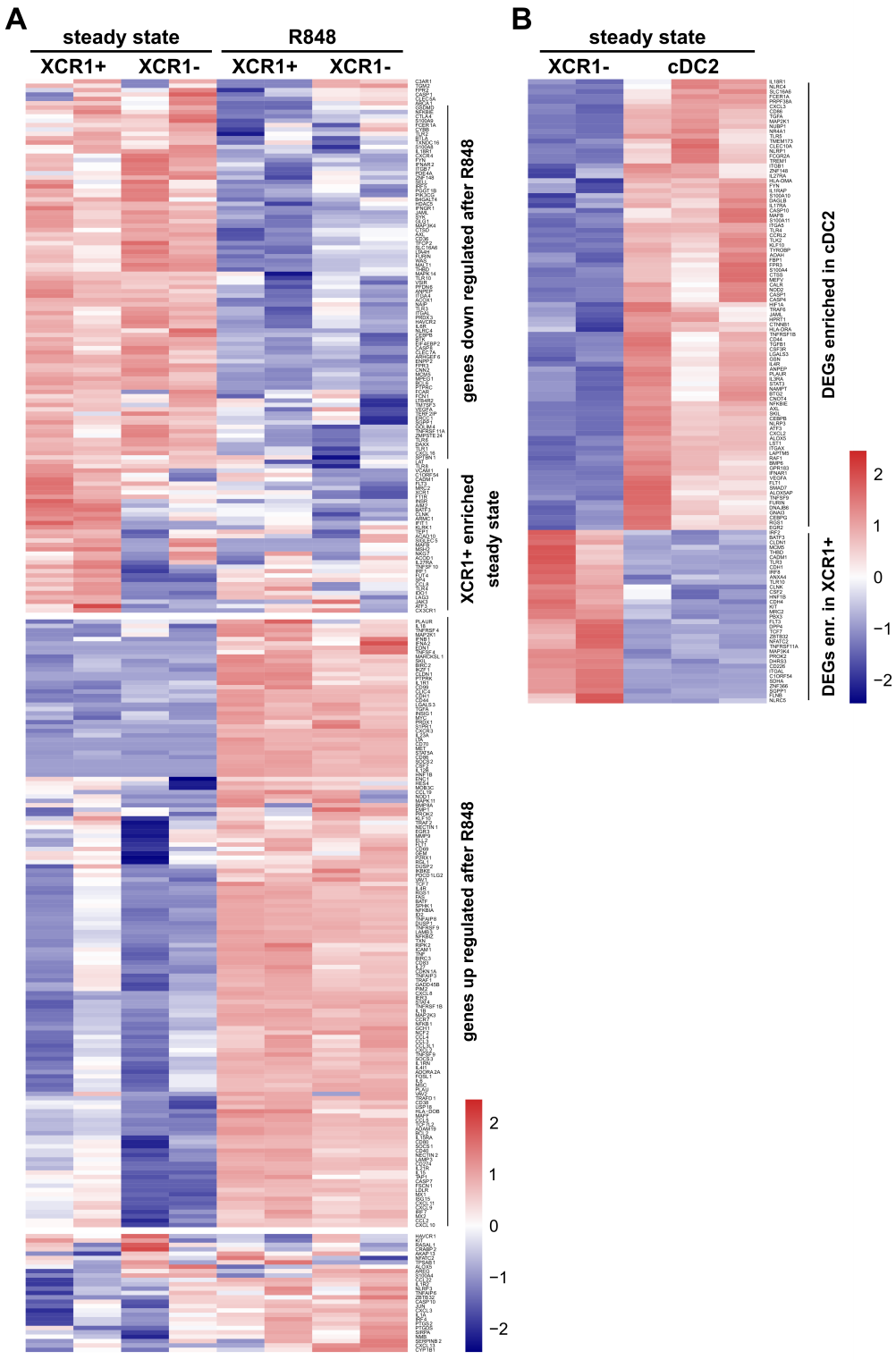

Fig. S5. Differentially expressed genes between XCR1$^-$ and XCR1$^+$ cDC1 in the steady state and after stimulation with R848. Blood DCs were enriched from PBMCs of healthy donors using the EasySep Pan-DC Pre-Enrichment Kit. XCR1$^-$ and XCR1$^+$ cDC1 were sorted as shown in Fig. S4. Subsequently, cells were stimulated or not with 5 µg/ml R848 for 3 h. mRNA expression of 800 genes was determined using NanoString technology (770 genes from the nCounter Human Myeloid

Innate Immunity V2 Panel and 30 DC- and inflammation-specific genes) as described before (4). A) Eight samples of 800 gene features were normalized by RUVg. mRNA data were then analyzed for differentially expressed genes (DEGs) using edgeR with a threshold of an FDR-adjusted P value of 0.01 and a log2FC of 1.5. All genes showing differential expression between the different groups were hierarchically clustered and plotted as heatmap. B) mRNA data of XCR1^{-} cDC1 were compared to published mRNA data of human cDC2 analyzed with the same Nanostring set (4). DEGs between XCR1^{-} cDC1 and cDC2 were hierarchically clustered and plotted as heatmap.

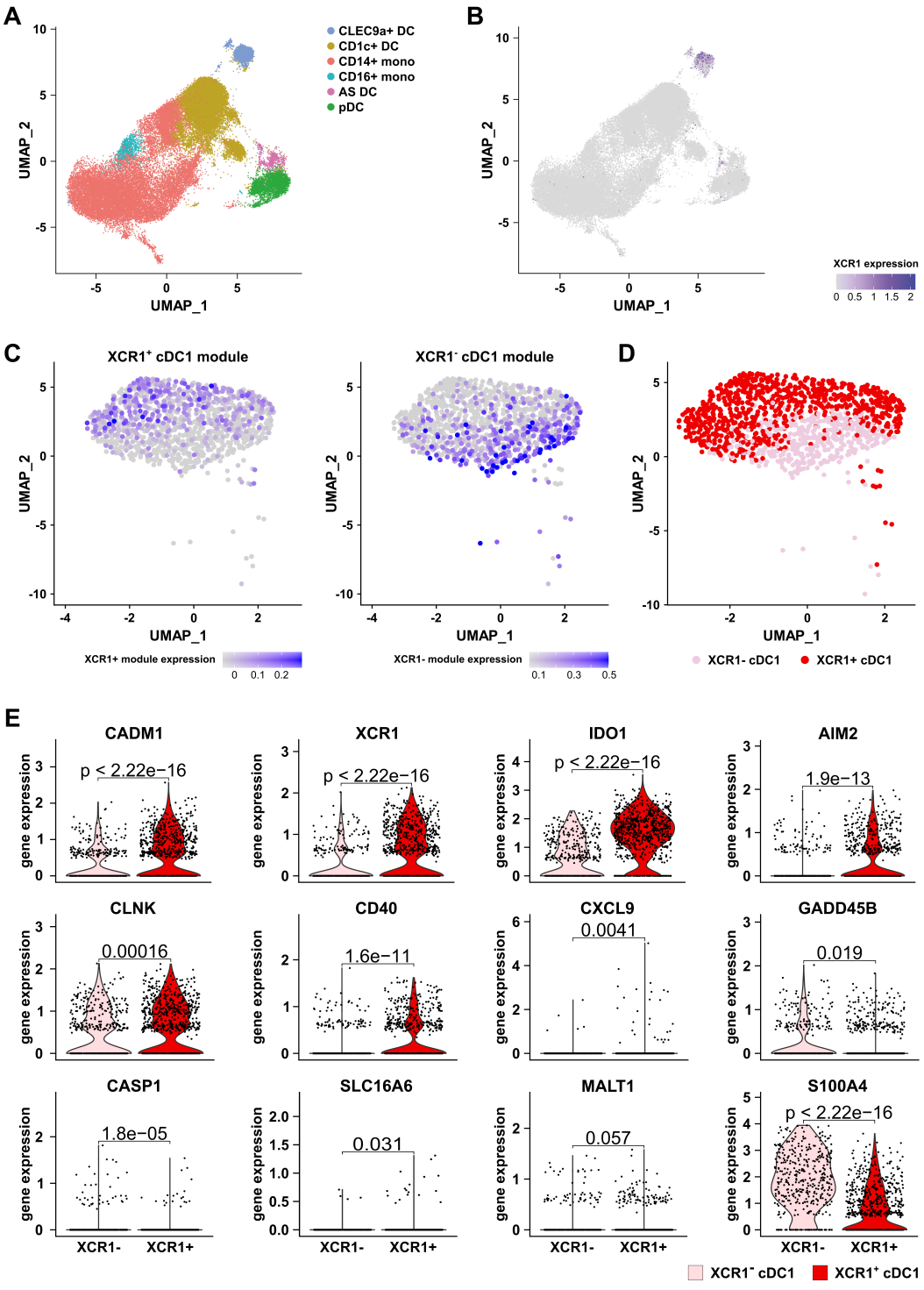

Fig. S6. XCR1⁻ and XCR1⁺ cDC1 identified in published scRNAseq data. Published scRNAseq data of Saichi et al. (Gene Expression Omnibus under accession code GSE169346) were analyzed and clustered using Seurat (5). A) UMAP overlaid with indicated cell types. B) Feature plot of XCR1 expression. C) Gene expression modular score per cell. Up-regulated DEGs (identified by Nanostring in Figure 2b) of XCR1⁺ and XCR1⁻ cDC1 were defined as XCR1⁺ cDC1 module and XCR1⁻ cDC1 module, respectively. The module scores were visualized on the feature plots. D) CLEC9a⁺ DCs were clustered into XCR1⁻ (rose) and XCR1⁺ (red) cDC1. E) Violin plots show

expression of selected DEGs- among XCR1^{-} cDC1 (rose) and XCR1^{+} cDC1 (red) as clustered in D), t-test *p* values are labeled in the figure.

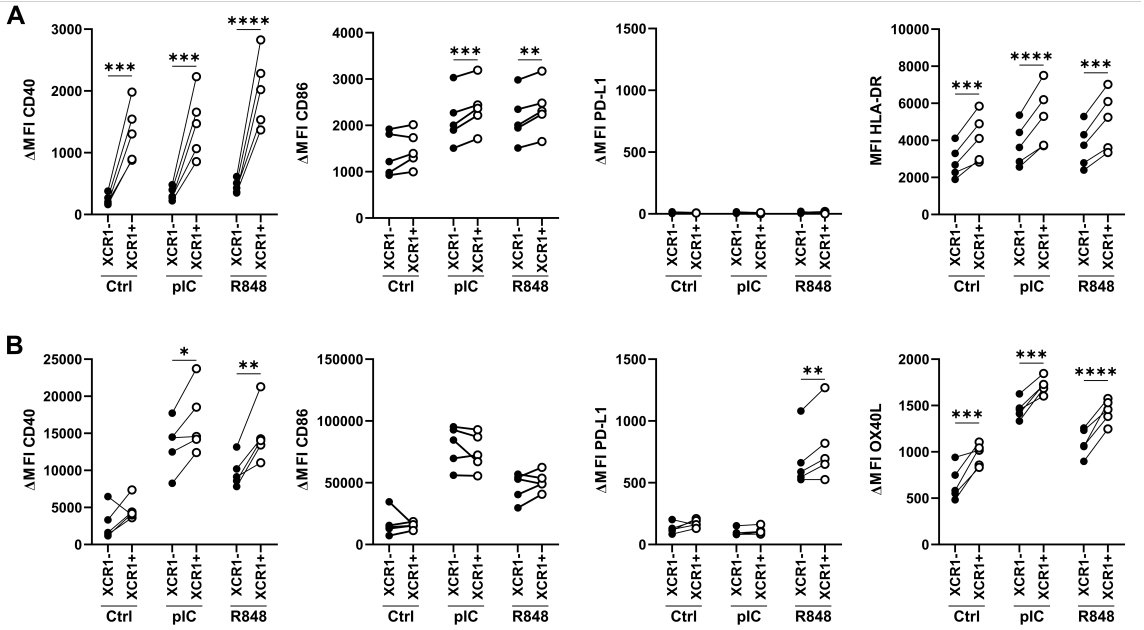

Fig. S7. Enhanced expression of co-stimulatory and -inhibitory molecules on human XCR1$^+$ cDC1 after TLR stimulation. Blood DCs were enriched from PBMCs of healthy donors using the EasySep Pan-DC Pre-Enrichment Kit. XCR1$^-$ and XCR1$^+$ cDC1 were sorted as shown in Fig. S4. Subsequently, cells were stimulated or not either with 5 µg/ml R848 or 5 µg/ml pIC for A) 3h or B) 12 h. Cells were harvested and analyzed for the expression of A and B) CD40 (clone: 5C3, A647, BioLegend), CD86 (clone: 2331 (FUN1), PE-CF594, BD Biosciences), PD-L1 (clone: MIH3, BV421, BioLegend), A) HLA-DR (clone. G46-6, BUV395, BD Biosciences) or OX40L (clone: 11C3.1, PE, BioLegend) in comparison to respective isotype controls by flow cytometry. Samples were acquired using a BD LSRFortessa and data analyzed using FlowJo software. Scatter plots depict ΔMFI values for CD40, CD86, PD-L1, and OX40L compared to isotype controls (ΔMFI value= MFI value experimental condition – MFI value isotype control) and MFI value for HLA-DR expression (black circles: XCR1$^-$ cDC1; open circles: XCR1$^+$ cDC1; individual donors connected by line; N=5; * p<0.05, ** p<0.01, *** p<0.01, **** p<0.001; two-way ANOVA).

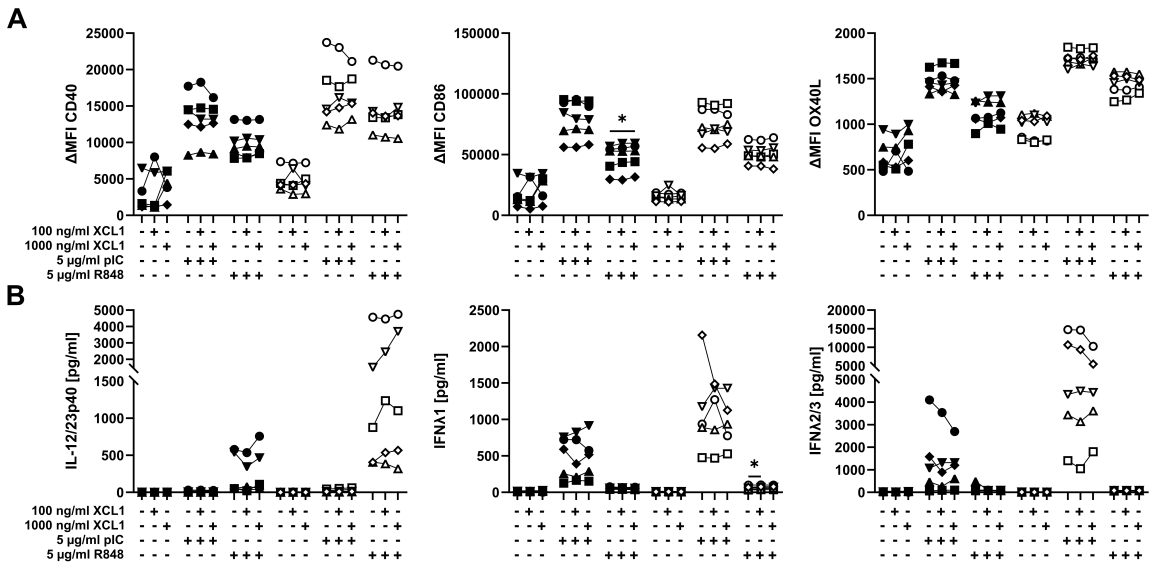

Fig. S8. Signaling of XCR1 does not influence activation and cytokine secretion of XCR1$^-$ and XCR1$^+$ cDC1. Blood DCs were enriched from PBMCs of healthy donors using the EasySep Pan-DC Pre-Enrichment Kit. XCR1$^-$ and XCR1$^+$ cDC1 were sorted as shown in Fig. S4. Subsequently, cells were stimulated or not either with 5 µg/ml R848 or 5 µg/ml pIC in presence of either 100 ng/ml or 1000 ng/ml XCL1 for 12h. A) Cells were harvested and analyzed for the expression of CD40 (clone: 5C3, A647, BioLegend), CD86 (clone: 2331 (FUN1), PE-CF594, BD Biosciences), and OX40L (clone: 11C3.1, PE, BioLegend) in comparison to respective isotype controls by flow cytometry. B) Supernatants of the cells were collected and stored at -80°C until analysis. Cytokines were determined using the LEGENDplex Human Anti-Virus Response Panel (BioLegend). Samples were acquired using a BD LSRFortessa and data analyzed using A) FlowJo software or B) LEGENDplex Software Suite. Scatter plots depict A) ΔMFI values for CD40, CD86, and OX40L compared to isotype controls (ΔMFI value= MFI value experimental condition – MFI value isotype control) and B) concentration of IL-12/IL-23p40, IFNλ1, and IFNλ2/3 (black symbols: XCR1$^-$ cDC1; open symbols: XCR1$^+$ cDC1; individual donors connected by line; N=5; * p<0.05, ** p<0.01, *** p<0.01, **** p<0.001; two-way ANOVA).

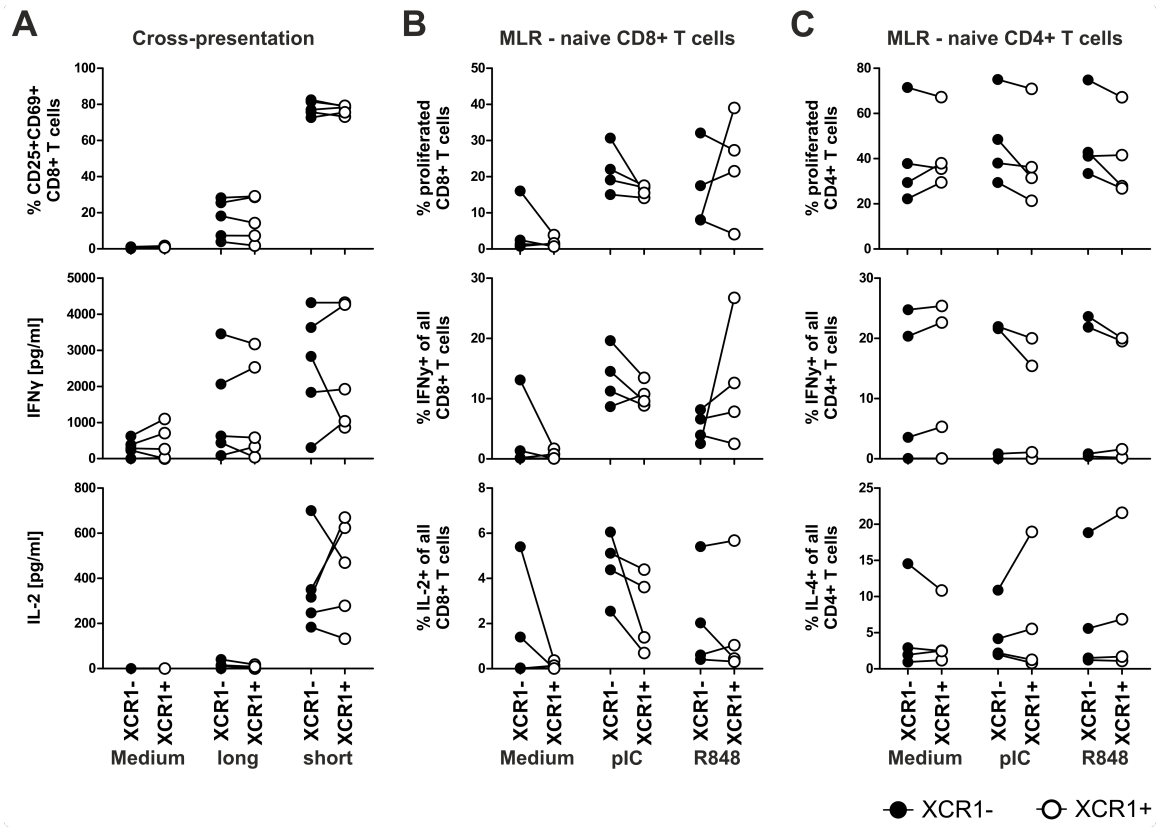

Fig. S9. XCR1$^-$ and XCR1$^+$ cDC1 show comparable capacity to induce T cell responses *in vitro*. Blood DCs were enriched from PBMCs of healthy donors using the EasySep Pan-DC Pre-Enrichment Kit. XCR1$^-$ and XCR1$^+$ cDC1 were sorted as shown in Fig. S4. A) CD8$^+$ T cells were isolated using the EasySep Human CD8+ T cell Isolation Kit, B) naïve CD8$^+$ T cells were isolated using the EasySep Human Naïve CD8+ T Cell Isolation Kit and C) naïve CD4$^+$ T cells were isolated using the EasySep Human Naïve CD4+ T Cell Isolation Kit. A) CD8$^+$ T cells were electroporated with the mRNA for a gp100-specific TCR. The electroporation was performed as described before (1–3). Then, XCR1$^-$ and XCR1$^+$ cDC1 were co-cultured with autologous TCR-transfected CD8$^+$ T cells in a 1:1 ratio for 18 h in presence or not either of a long or short gp100 peptide. CD8$^+$ T cells were analyzed for the expression of activation marker (CD25, CD69) by flow cytometry and concentration of IFNγ and IL-2 were determined in the SN by CBA assay (CBA Flex-Sets). B-C) XCR1$^-$ and XCR1$^+$ cDC1 were stimulated or not with 5 µg/ml R848 or pIC for 3 h. After washing, cells were co-cultured with HLA-mismatched CFSE-labeled naïve B) CD8$^+$ or C) CD4$^+$ T cells of different blood donor in a 1:10 (DC:T cell) ratio for 7d. After seven days, T cells were restimulated with PMA/Ionomycin in presence of Brefeldin A for 6 h. Then, cells were analyzed by intracellular flow cytometry for proliferation (dilution of CFSE), activation (CD25) and phenotype (intracellular cytokines). A-C) Samples were acquired using a BD LSRFortessa and data analyzed using FlowJo or FCAP array V3 (Cytokines in A). Data are plotted as scatter plots (filled circles: XCR1$^-$ cDC1; open circles: XCR1$^+$ cDC1; individual donors connected by lines; A) N=5, B-C) N=4).

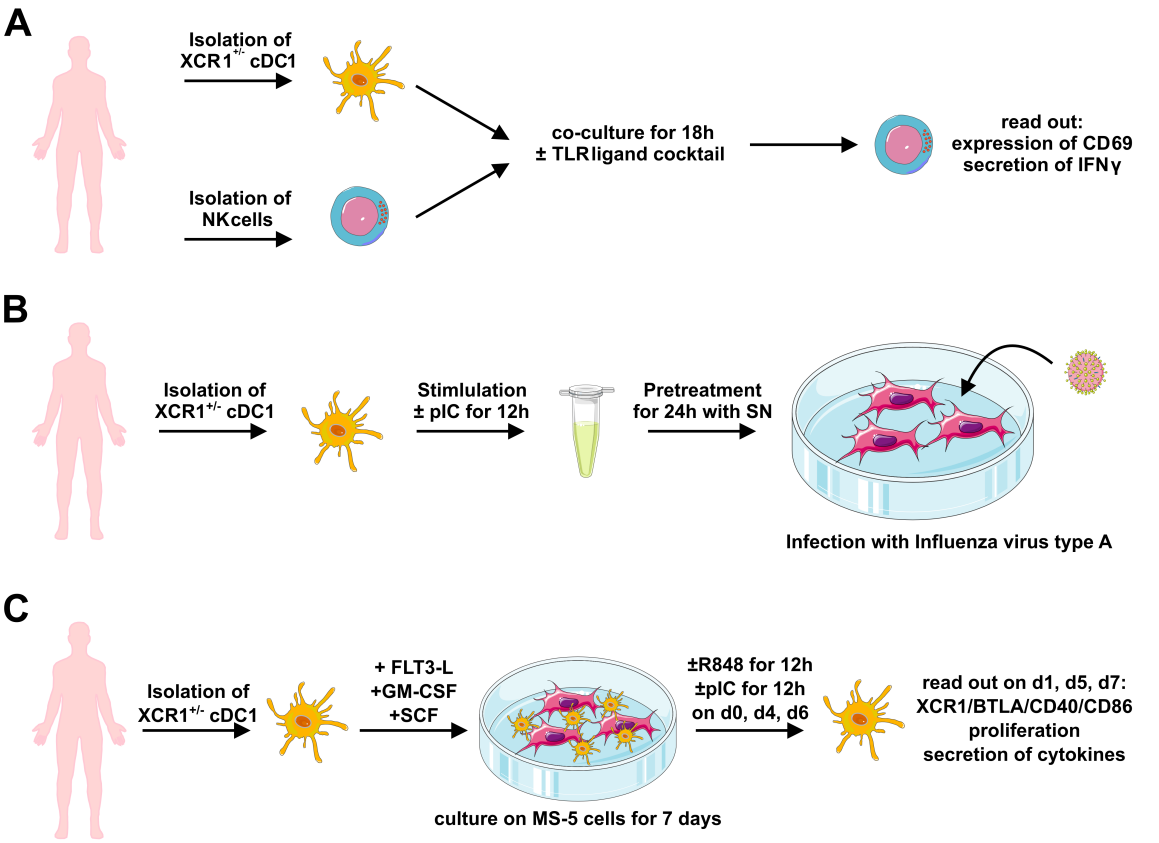

Fig. S10. Experimental schemes. A) Scheme for co-culture assay of XCR1$^-$ and XCR1$^+$ cDC1 with NK cells of the same donor. XCR1$^-$ and XCR1$^+$ cDC1 were sorted from DC-enriched PBMCs as described before. NK cells were enriched by depletion of unwanted cells and sorted as CD56+CD335+. Subsequently, XCR1$^-$ or XCR1$^+$ cDC1 were co-cultured with NK cells in a 1:5 ratio in presence or not of 2.5 µg/ml R848, 2.5 µg/ml pIC and 2.5 µg/ml CpG (Type A). After 18 h, supernatants were harvested and analyzed for the secretion of IFNγ by CBA Flex-Set (BD Biosciences) as well as NK cells for the expression of CD69 by flow cytometry. Samples were acquired using a BD LSRFortessa and analyzed using FlowJo (CD69 expression) or FCAP Array 3.1 (IFNγ secretion). B) Scheme for inhibition of viral replication assay. XCR1$^-$ and XCR1$^+$ cDC1 were sorted and subsequently stimulated or not with 5 µg/ml pIC for 3 h. After washing, cells were cultured for 12 h. Then, supernatants (SN) were harvested and used for the pretreatment of U2OS cells. After overnight culture, U2OS cells were challenged with luciferase-expressing Influenza virus type A (strain PR8-Luc). C) Experimental setup for DC differentiation assay. XCR1$^-$ and XCR1$^+$ cDC1 were sorted from the blood of healthy donors and labeled with 5µM Celltrace Violet. Subsequently, cells were cultured on MS-5 stroma cells for 7 d in presence of 800 ng/ml FLT3L, 160 ng/ml SCF and 160 ng/ml GM-CSF. On days 0, 4, and 6, cells were stimulated for 12 h or not with either 5 µg/ml pIC or R848. SN were harvested and cells were analyzed by flow cytometry for XCR1, BTLA, CD40, and CD86 expression. SN were analyzed for cyto- and chemokine secretion by CBA assay (LEGENDplex Human Anti-Virus Response Panel). Samples were acquired using a BD LSRFortessa and data were analyzed with FlowJo (XCR1, CD40, CD86) or LEGENDplex software suit (Cyto- and chemokine secretion). B-C) Parts of the images are provided and adapted from Servier Medical Art (smart.servier.com) and are licensed under the Creative Commons Attribution 3.0 Unported License (creativecommons.org/ licenses/by/3.0/).

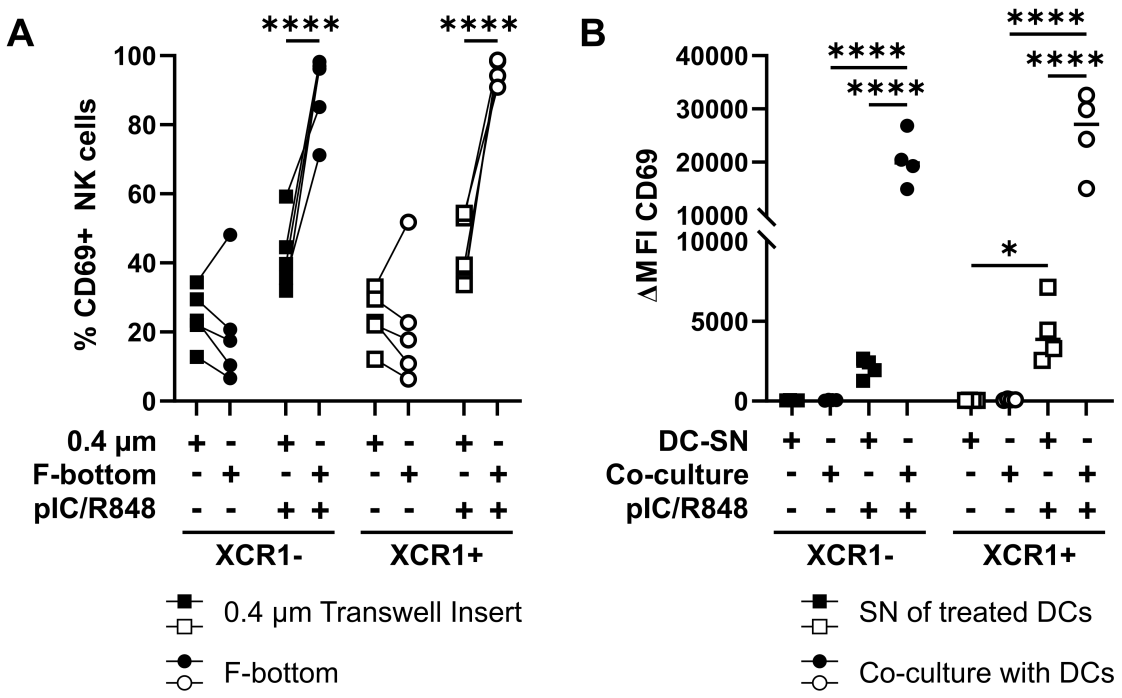

Fig. S11. Direct interaction of XCR1$^+$ and XCR1$^-$ cDC1 is necessary for full activation of NK cells. A and B) XCR1$^-$ and XCR1$^+$ cDC1 were sorted from DC-enriched PBMCs as described before. NK cells were enriched by depletion of T cells, B cells and monocytes by biotinylated antibodies (anti-CD3, anti-CD19, anti-CD14) followed by restraining in a magnet using Streptavidin-coated nanobeads (BioLegend). Enriched NK cells were sorted as CD56$^+$CD335$^+$. A) XCR1$^-$ or XCR1$^+$ cDC1 were co-cultured with NK cells in a 1:5 ratio in presence or not of 2.5 µg/ml R848 and 2.5 µg/ml pIC in a 96-well F-bottom plate or separated by a 0.4 µm Transwell insert. B) XCR1$^-$ and XCR1$^+$ cDC1 were stimulated with 2.5 µg/ml R848 and 2.5 µg/ml pIC or kept in medium for 12h. Supernatants were collected and stored at -80°C until usage. Sorted NK cells were either directly co-cultured with XCR1$^+$ or XCR1$^-$ cDC1 at 1:5 ratio in presence or not of 2.5 µg/ml R848/pIC or cultured in supernatant of stimulated DCs (volume contains cytokines of the same number of DCs as used in the direct co-culture). A and B) After 18 h, NK cells were harvested and analyzed for the expression of CD69 by flow cytometry. Samples were acquired using a BD LSRFortessa and analyzed using FlowJo. Scatter plots show A) % CD69$^+$ NK cells or B) ΔMFI for CD69 ((A) N=5, (B) N=4, each donor connected by line). * p<0.05, ** p<0.01, *** p<0.01, **** p<0.001; two-way ANOVA.

Supporting Tables

Table S1: Antibody panel for analysis of XCR1 expression on human immune cells

Fluorophore/Labelling	Antigen	Clone	Company	Dilution
BUV395	CD3	UCHT1	BD Biosciences	1:100
BUV737	CD8	SK1	BD Biosciences	1:100
BV421	CD56	5.1H11	BioLegend	1:100
	CD335	2H9	BioLegend	1:200
BV510	CD4	OKT4	BioLegend	1:100
BV605	CD19	SJ25C1	BioLegend	1:100
	CD20	2H7	BioLegend	1:200
BV650	CD123	6H6	BioLegend	1:100
BV711	CD141	1A4	BD Biosciences	1:100
FITC				
PerCP/Cy5.5	CD303	201A	BioLegend	1:100
PE	XCR1	S15046E	BioLegend	1:100
PE-CF 594	HLA-DR	G46-6	BD Biosciences	1:200
PE/Cy5	CD11b	M1/70	BioLegend	1:1000
PE/Cy7	CD11c	3.9	BioLegend	1:100
APC				
A700	CD14	M5E2	BioLegend	1:100
APC/Fire 750	CD1c	L161	BioLegend	1:100
-	Trustain FcX	-	BioLegend	1:50

Table S2: Antibody panel for analysis of XCR1 expression on cells in human lung

Fluorophore/Labelling	Antigen	Clone	Company	Dilution
BUV395	HLA-DR	G46-6	BD Biosciences	1:100
BUV737	CD14	M5E2	BD Biosciences	1:100
BV421	CD3	UCHT1	BioLegend	1:100
BV510	CD11c	S-HCL-3	BioLegend	1:100
BV605	CD19	SJ25C1	BioLegend	1:100
	CD20	2H7	BioLegend	1:200
BV650	CD123	6H6	BioLegend	1:100
BV711	CD5	UCHT2	BioLegend	1:100
FITC				
PerCP/Cy5.5	CD303	201A	BioLegend	1:100
PE	XCR1	S15046E	BioLegend	1:100
PE/Dazzle594	CD163	GHI/61	BioLegend	1:200
PE/Cy7	CD141	M80	BioLegend	1:100
APC	CLEC9A	8F9	BioLegend	1:100
A700	CD45	HI30	BioLegend	1:100
APC/Fire 750	CD1c	L161	BioLegend	1:100
-	Trustain FcX	-	BioLegend	1:50

Table S3: Antibody panel for sorting of human DC subpopulations with PE-coupled anti-XCR1 antibody

Fluorophore/Labeling	Antigen	Clone	Company	Dilution
BUV395	CD3	UCHT1	BD Bioscience	1:100
BV421	CD19	HIB19	BioLegend	1:200
	CD20	2H7	BioLegend	1:200
	CD56	5.1H11	BioLegend	1:200
BV510	HLA-DR	L243	BioLegend	1:100
BV605	CD123	6H6	BioLegend	1:100
BV711	CD141	1A4	BD Biosciences	1:100
PerCP/Cy5.5	CD303	201A	BioLegend	1:100
PE	XCR1	S15046E	BioLegend	1:100
PE/Cy7	CD11c	3.9	BioLegend	1:100
A700	CD14	M5E2	BioLegend	1:200
APC/Fire 750	CD1c	L161	BioLegend	1:100

Table S4: Antibody panel for sorting of human DC subpopulations with FITC-coupled anti-XCR1 antibody

Fluorophore/Labeling	Antigen	Clone	Company	Dilution
BUV395	HLA-DR	G46-6	BD Bioscience	1:100
BV421	CD3	UCHT1	BioLegend	1:200
	CD19	HIB19	BioLegend	1:200
	CD20	2H7	BioLegend	1:200
	CD335	2H9	BioLegend	1:200
BV510	CD11c	S-HCL-3	BioLegend	1:100
BV605	CD141	M80	BioLegend	1:100
FITC	XCR1	S15046E	BioLegend	1:100
PerCP/Cy5.5	CD163	GHI/61	BioLegend	1:100
PE	CD64	10.1	BioLegend	1:100
PE/Cy5	CD123	6H6	BioLegend	1:200
A700	CD14	M5E2	BioLegend	1:200
	CD88	S5/1	BioLegend	1:200
APC/Fire 750	CD1c	L161	BioLegend	1:100

Table S5: Used antibodies for high dimensional analysis of the blood DC compartment

Fluorophore/Labelling	Antigen	Clone	Company	Dilution
BUV395	HLA-DR	G46-6	BD Biosciences	1:100
BUV737	CD14	M5E2	BD Biosciences	1:100
BV421	CD3	UCHT1	BioLegend	1:100
	CD19	HIB19	BioLegend	1:200
	CD20	2H7	BioLegend	1:200
	CD56	5.1H11	BioLegend	1:200
	CD335	2H9	BioLegend	1:200
BV510	CD11c	S-HCL-3	BioLegend	1:100
BV605	CD141	M80	BioLegend	1:100
BV650	CD123	6H6	BioLegend	1:100
FITC	XCR1	S15046E	BioLegend	1:100
PerCP/Cy5.5	CD303	201A	BioLegend	1:100
PE (one per sample)	CD5	UCHT2	BioLegend	1:100
	CD13	WM15	BioLegend	1:100
	CD26	BA5b	BioLegend	1:100
	CD205	MG38	BD Biosciences	1:50
	CD226	11A8	BioLegend	1:100
	CLEC7A (Dectin-1)	15E2	BioLegend	1:100
PE/Dazzle594	CD163	GHI/61	BioLegend	1:200
PE/Cy5	BTLA	MIH26	BioLegend	1:100
PE/Cy7	Axl	DS7HAXL	eBioscience	1:100
APC	CLEC9A	8F9	BioLegend	1:100
A700	CD88	S5/1	BioLegend	1:100
	CD89	A59	Biolegend	1:100
APC/Fire 750	CD1c	L161	BioLegend	1:100
-	Trustain FcX	-	BioLegend	1:50

SI References

1. N. Schaft, *et al.*, A new way to generate cytolytic tumor-specific T cells: electroporation of RNA coding for a T cell receptor into T lymphocytes. *Cancer Immunol. Immunother.* **55**, 1132–1141 (2006).
2. S. Hoyer, *et al.*, Braf and mek inhibitors affect dendritic-cell maturation and t-cell stimulation. *Int. J. Mol. Sci.* **22** (2021).
3. K. F. Gerer, S. Hoyer, J. Dörrie, N. Schaft, Electroporation of mRNA as Universal Technology Platform to Transfect a Variety of Primary Cells with Antigens and Functional Proteins. *Methods Mol. Biol.* **1499**, 165–178 (2017).
4. L. Hatscher, *et al.*, Select hyperactivating NLRP3 ligands enhance the T H 1- and T H 17-inducing potential of human type 2 conventional dendritic cells. *Sci. Signal.* **14**, eabe1757 (2021).
5. M. Saichi, *et al.*, Single-cell RNA sequencing of blood antigen-presenting cells in severe COVID-19 reveals multi-process defects in antiviral immunity. *Nat. Cell Biol.* **23**, 538–551 (2021).